J Incl Phenom Macrocycl Chem (2011) 71:419–428
DOI 10.1007/s10847-011-9976-8

ORIGINAL ARTICLE

TD-DFT computations for trigonal silicon(IV) coordination compounds of rigid bidentates

Sven E. Harnung · Erik Larsen

Received: 12 April 2011 / Accepted: 23 April 2011 / Published online: 12 May 2011

Abstract Computations using standard time dependent DFT (B3LYP/6-31G) can neither reproduce experimental CD spectra of optically active tris(2,4-pentanedionato)silicon(IV), $[Si(acac)_3]^+$, nor the CD of a series of similar coordination compounds of Si(IV). These compounds are characterized by exciton coupled ligand transitions which are not influenced by orbitals on the central ion. We have found that TD DFT calculations using long range functionals can indeed reproduce the measured CD satisfactorily. The detailed interpretations make use of D_3 point group symmetry and symmetry adapted excited state functions allowing for the electronic coupling of the excitation of the ligands. Computations of similar problems for transition metal ions coordinated to rigid π systems are common and probably also sensitive to the choice of functional.

Keywords Time dependent-density functioanl theory, TD-DFT · Test of functionals · Circular dichroism, CD · Tris(acetylacetonato)silicon(IV) ion · Tris(tropolonato)silicon(IV) ion · Tris(bipyridine)silicon(IV) ion

Dedicated to Professor Leonard F. Lindoy, a pioneer of macrocyclic and supramolecular chemisttry, on the occasion of his 75th birthday.

S. E. Harnung
Department of Chemistry, University of Copenhagen, Universitetsparken 5, 2100 Copenhagen, Denmark
e-mail: harnung@kiku.dk

E. Larsen (✉)
IGM, Faculty of Life Sciences, University of Copenhagen, Thorvaldsensvej 40, 1871 Frederiksberg, Denmark
e-mail: erik@life.ku.dk

Introduction

Trigonally structured coordination compounds such as compounds made of ligands like 2,4-pentanedionate (acetylacetonate, $acac^-$), oxalate (ox^{2-}), and phenanthroline (phen) have been used extensively in studies of chiral coordination compounds. Most often central ions of the first transitional group elements have been chosen but also simpler entities like $[Si(acac)_3]^+$ and $[Si(tropolonate)_3]^+$ have been studied [1–3]. These ions have no d-orbitals and the electronic interaction between the ligand π system and the central ion orbitals are weak such that the UV–Vis and CD spectra are undisturbed by intense charge transfer bands. Density functional theory has proven to be useful and reliable when applied to calculation of properties of the electronic ground state. Thus Lindoy and coworkers has used DFT to calculate energies of isomers of low-spin $[Ni(cyclam)]^{2+}$ and investigated the role of copper(II) in the Maillard reaction and Kapinos and coworkers have successfully computed relative acidities of hydrogen adenosine [4–7]. We wish to use time-dependent DFT to calculate properties of the excited states of the mentioned silicon(IV) coordination compounds and this seems possible in view of earlier work on excited states of coordination compounds [8–10]. It should be possible to study the electrostatic coupling between the three ligands because the spectral contributions are solely from the ligands. Therefore we can test the results produced by exciton theory on weak electronic interactions and thereby check if the software treats the symmetry requirements correctly. As shown below this is not the case for TD-DFT computations using the most popular functional B3LYP.

Computational details

DFT computations were performed with Gaussian09 version B.01 [11] with standard functionals and basis sets. Time-dependent DFT was used to compute excited state energies and transition moments. The energies of up to 40 excited states were estimated to cover the considered wavelength range 400–180 nm. Computations were performed with and without symmetry adaptions to ensure correct results. The computed rotatory strengths based on velocity dipoles have been converted to gaussian shaped CD spectra using a Mathematica® routine or a spreadsheet.

The circular dichroism $\Delta\varepsilon_K(\omega)$ of the K'th electronic transition may be given by the expression

$$\frac{\Delta\varepsilon_K(\omega)}{\omega} = \gamma R_K \rho(\omega - \omega_K).$$

The constant γ is given by

$$\gamma = \frac{4\pi N_A \lg(e)}{3\hbar c_0^2 \varepsilon_0} = 1.30544 \times 10^{52} \frac{1\ \mathrm{T\,m^2}}{\mathrm{Cm\,J\,mol}}$$

and R_K is the rotatory strength which with this choice of units has the unit (Cm)(J/T). The bell-shaped function ρ is not necessarily symmetrical. Therefore it may be characterized in terms of moments and reproduced by expansion onto Hermite polynomia [12]:

The integral of the function ρ in an interval around some characteristic frequency is unity,

$$\int_{\omega_K-\eta}^{\omega_K+\eta} \rho(\omega)\mathrm{d}\omega = 1$$

The υth moment is defined by

$$\mu_{K,\upsilon} = \int_{\omega_K-\eta}^{\omega_K+\eta} (\omega - \omega_K)^{\upsilon} \rho(\omega)\mathrm{d}\omega$$

where ω_K is the mean frequency, defined by the condition $\mu_{K,1} = 0$, and $\mu_{K,2} = (\Delta\omega_K)^2$ is the square width.

Experimentally the rotatory strength is found by integration of the circular dichroism spectrum:

$$\begin{aligned} R_K &= \frac{1}{\gamma} \int_{\omega_K-\eta}^{\omega_K+\eta} \frac{\Delta\varepsilon(\omega)}{\omega}\mathrm{d}\omega \\ &= 7.66026 \times 10^{-53}\,\mathrm{C\ m\ J\ T^{-1}} \int_{\omega_K-\eta}^{\omega_K+\eta} \frac{\Delta\varepsilon_K(\omega)}{\mathrm{m^2 mol^{-1}}}\,\mathrm{d}\ln\omega \\ &= 2.29649 \times 10^{-40}\,\mathrm{Fr\ cm\ erg\ G^{-1}} \int_{\omega_K-\eta}^{\omega_K+\eta} \frac{\Delta\varepsilon_K(\omega)}{\mathrm{m^2 mol^{-1}}}\,\mathrm{d}\ln\omega \end{aligned}$$

and R_K plays the role of normalizing the moments [12]. On this background the CD-spectrum may be drawn from the calculated rotatory strengths as a sum of gaussian lineshape curves

$$\Delta\varepsilon(\omega) = \frac{\omega}{22.9649 \times 10^{-40}} \sum_i^N \frac{1}{\Delta\omega_i\sqrt{2\pi}} \frac{R_i}{\mathrm{Fr\ cm\frac{erg}{G}}} \times \exp\left(-\frac{(\omega-\omega_i)^2}{2(\Delta\omega_i)^2}\right) \mathrm{M^{-1}cm^{-1}}$$

using cgs-units for R_i and the unit l/(M cm) for $\Delta\varepsilon$.

The width of the Gaussian components, $\Delta\omega$, is 0.12 μm^{-1} everywhere. We have chosen always to draw the calculated curves without offset or scaling. It is a general experience that TD-DFT computed transition energies are larger than the experimentally observed ones. In case of the silicon(IV) coordination compounds dealt with here the computed values are 0.4–0.5 μm^{-1} larger than the experimental values, and we consider this to be a close resemblance.

Symmetry considerations

We will deal with coordination compounds of three symmetric, planar and conjugated ligands having the D_3 point group symmetry and thus the capability to exist as a chiral pair of Δ and Λ configuration [13]. To focus the discussion we will discuss and present only values for the Λ isomer of the compounds.

The ligand π orbitals as represented by a vector (the p-orbital) on the ligating atoms are shown in Fig. 1 top, where the three ligands span the coordination sites 1,4; 2,6; and 3,5. The ligand π orbitals are also sketched in this figure in the form of the two possible groups of π frontier ligand orbitals being either antisymmetrical (ψ) or symmetrical (χ) with respect to rotation around a line passing through the central ion and the midpoint of the ligand. The characterization of the πMOs as ψ or χ was suggested by Orgel already in 1961 [14]. In Fig. 1 bottom the ψ and χ character is demonstrated again and in the two drawings we have chosen to depict the case where the ligating atoms occupy the ideal octahedral positions. This is by no means a necessary condition but chosen in order to show that even in this case the coordination compound is of true D_3 symmetry. The two drawings to the left depict a molecular orbital of a_2 symmetry while the two drawings to the right an orbital of a_1 symmetry in D_3. They can be written for the HOMO and LUMO from the origin using the barred coordination system:

T_{1u} octahedral states	T_{2g} octahedral states
$\Psi^{3\pi}(a_2) = \frac{1}{\sqrt{3}}(\psi_a + \psi_b + \psi_c)$.	$\Psi^{4\pi}(a_1) = \frac{1}{\sqrt{3}}(\chi_a + \chi_b + \chi_c)$ and
the corresponding orbitals with e symmetry are	
$\Psi^{3\pi}(e_{\bar{x}}) = \frac{1}{\sqrt{6}}(2\psi_a - \psi_b - \psi_c)$	$\Psi^{4\pi}(e_{\bar{x}}) = \frac{1}{\sqrt{2}}(-\chi_b + \chi_c)$
$\Psi^{3\pi}(e_{\bar{y}}) = \frac{1}{\sqrt{2}}(\psi_b - \psi_c)$	$\Psi^{4\pi}(e_{\bar{y}}) = \frac{1}{\sqrt{6}}(2\chi_a - \chi_b - \chi_c)$

Discussion

Density functional theory computations of $[Si(acac)_3]^+$. DFT is well suited for theoretical description of coordination compounds of metal ions surrounded by three planar, conjugated ligands. Here it is shown that computations on the tris(2,4-pentanedionato)silicon(IV) ion, $[Si(acac)_3]^+$ result in relative unperturbed π-ligand Kohn–Sham orbitals. The central ion has in this case no d-electrons and overlaps between its s and p orbitals with the ligand π orbitals are very small. The ion $[Si(acac)_3]^+$ was first reported in 1903[15] and resolved into enantiomers 1959 [2]. The absolute configuration of the $(-)_D$ stereoisomer was determined from the circular dichroism to be Δ [1]. This determination was based on empirical considerations of the exciton coupling of the $3\pi \rightarrow 4\pi$ transition of the ligands.

The standard computation with B3LYP functional and the 6-31G orbital set allows all ligand π orbitals to be recognized and also the silicon 3s and 3p orbitals are clearly identified. In Table 1 this is shown for the pertinent orbitals. The TD-DFT calculation has provided the orbital picture of the HOMOs and LUMOs shown in Fig. 2, and these orbitals show how the simple coupling scheme suggested in 1966 [1] show up undisturbed by overlap between ligand π and metal π orbitals. Note that the orbitals in Fig. 2 do look like the formally written a_1, a_2, and e combinations.

The experimentally obtained CD for $(-)_D$-$[Si(acac)_3]^+$ has been inverted to represent the CD of the $(+)_D$ stereoisomer which has the Λ configuration. It is depicted in Fig. 3 together with the CD computed for Λ-$[Si(acac)_3]^+$ with the functional B3LYP. From Fig. 3 it is obvious that the conclusion drawn on the absolute configuration (Δ) was correct since the computed CD of the Λ isomer has a mirror image relation to the experimental one. The computed result is displaced ca. 0.4 μm^{-1} at higher energies compared to the experimental one. The width used in constructing the computed CD curve seems to take a value between 0.12 and 0.2 μm^{-1}. We have chosen to use the value 0.12 μm^{-1} because this gives a close resemblance between experimental and computed absorption. Table 2 lists the singlet transitions calculated by TD-DFT and characterizes their dominating origins.

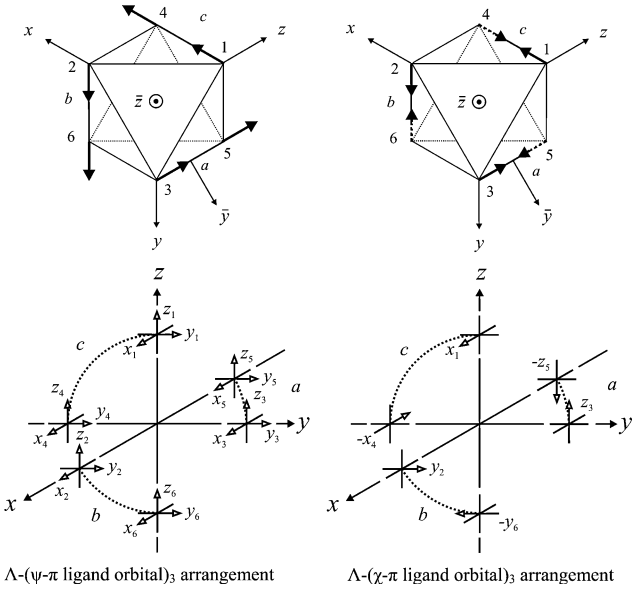

Fig. 1 Representations of the Λ diastereomer of a tris(bidentate) ligand coordination compound. *Upper panel*: The left hand figure shows a representation of the ligand molecular orbital $\Psi^{4\pi}(a_1)$ similarly, the right figure shows $\Psi^{3\pi}(a_2)$. The set of coordinate axes (x, y, z) go through the ligators whereas the set ($\bar{x}$, $\bar{y}$, $\bar{z}$) reflects the symmetry elements of the D_3 point group. The two coordinate systems are connected by the orthogonal substitution $\begin{bmatrix} e_{\bar{x}} \\ e_{\bar{y}} \\ e_{\bar{z}} \end{bmatrix} = \begin{bmatrix} \frac{1}{\sqrt{6}} & \frac{1}{\sqrt{6}} & \frac{-2}{\sqrt{6}} \\ \frac{-1}{\sqrt{2}} & \frac{1}{\sqrt{2}} & 0 \\ \frac{1}{\sqrt{3}} & \frac{1}{\sqrt{3}} & \frac{1}{\sqrt{3}} \end{bmatrix} \begin{bmatrix} e_x \\ e_y \\ e_z \end{bmatrix}$. Where e_i denotes unit vectors. *Lower panel*: The local coordinate system of the frontier orbitals $\Psi^{3\pi}(a_2)$ (left hand side) and $\Psi^{4\pi}(a_1)$ (right hand side). They are all parallel to the coordinate system (x, y, z)

Table 1 Characterization of selected molecular orbitals in $[Si(acac)_3]^+$

Orbital number	$\frac{E}{E_h}$	$\frac{E}{\mu m^{-1}}$	Origin (symmetry)
101, 102	0.034	0.746	3p(e) ψ
100	0.022	0.483	3p(a_2) ψ
93	−0.064	−1.405	5π(a_2) ψ
91, 92	−0.065	−1.427	5π(e) ψ
90	−0.073	−1.602	3 s-σ_L(a_1)
88, 89	−0.185	−4.060	4π(e) χ
87	−0.196	−4.302	4π(a_1) χ
86	−0.369	−8.099	3π(a_2) ψ
84, 85	−0.373	−8.186	3π (e) ψ
83–78			σ_L
76, 77	−0.477	−10.469	2π(e) χ
75-73			σ_L
72	−0.500	−10.974	2π(a_1) χ
71–57			σ_L
56	−0.570	−12.510	1π(a_2) ψ
54, 55	−0.579	−12.707	1π(e) ψ

Calculated with B3LYP/6-31+G(2df,p). Orbitals 84–89 from a B3LYP/6-31G calculation are shown in Fig. 2

$E_h = 219474.6\ cm^{-1} = 21.94746\ \mu m^{-1}$

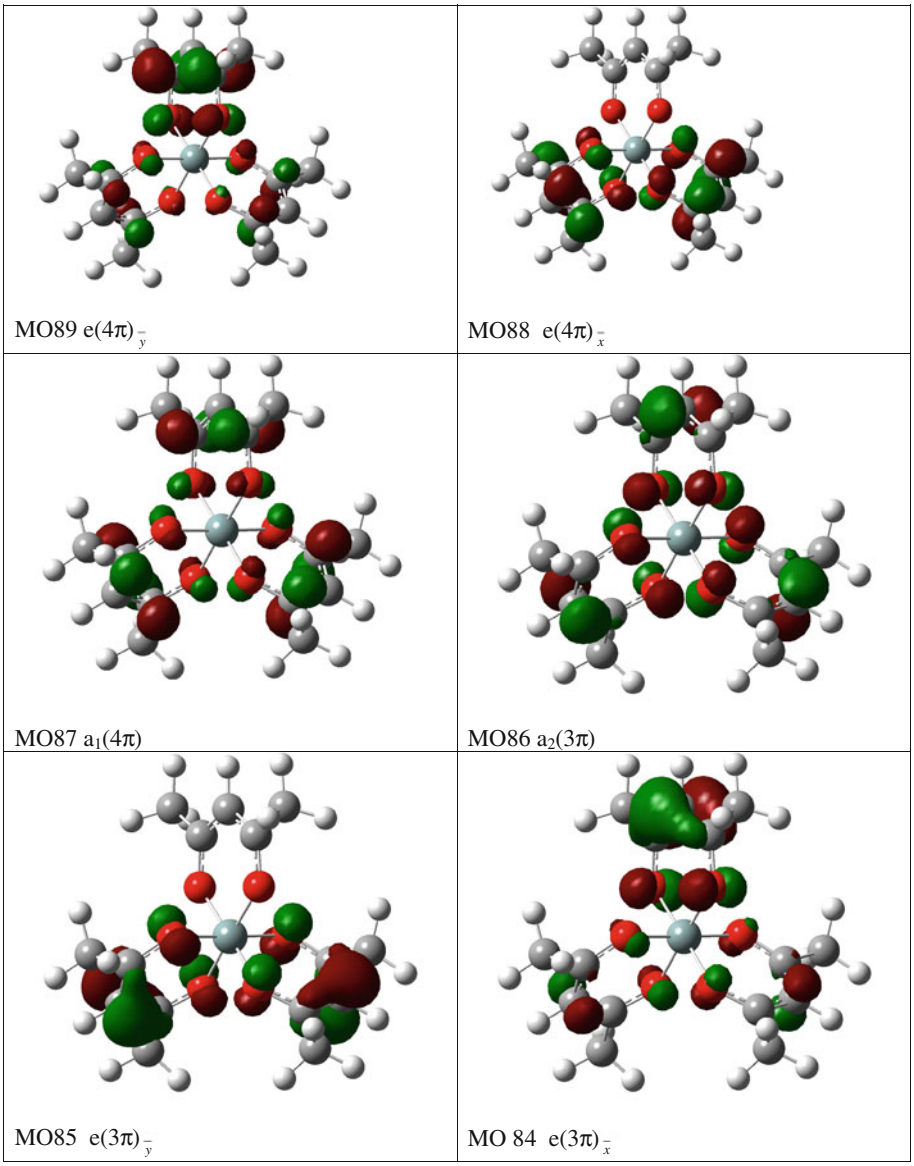

Fig. 2 LUMO and HOMO for Λ-$[Si(acac)_3]^+$. The drawings are constructed by GaussView 4.01 from orbitals obtained by B3LYP/6-31G functional and basis functions, constructed with cubes with npts = 81,75,64, isovalue = 0,050 and density 0.00040. O atoms are *red*, C *grey* and Si *light blue*

The $3\pi \rightarrow 4\pi$ transitions are computed (with B3LYP/6-31G) to be around 260 nm and there are several less intense transitions calculated to be at higher wavelengths. These transitions also have relatively low absorption and CD intensities (see Table 2) and they are not observed as independent transitions in absorption or CD. The set of $3\pi \rightarrow 4\pi$ transitions to states 1, 2, 3, 4, 5, 6, 10, 11 and 12 are further characterized by the help of Table 3. The $3\pi \rightarrow 4\pi$ exciton transitions used for the determination of the absolute configuration are the transitions to states 10–12. A more detailed list of the nine $3\pi \rightarrow 4\pi$ transitions as calculated by TD-DFT with B3LYP functional is shown in Table 3.

The results shown in Table 3 give a reminiscence of a coupling scheme where $|(3\pi e_x)^2\ (3\pi e_y)^2\ (3\pi a_2)^2|$ is the ground state written as a Slater determinant. The following

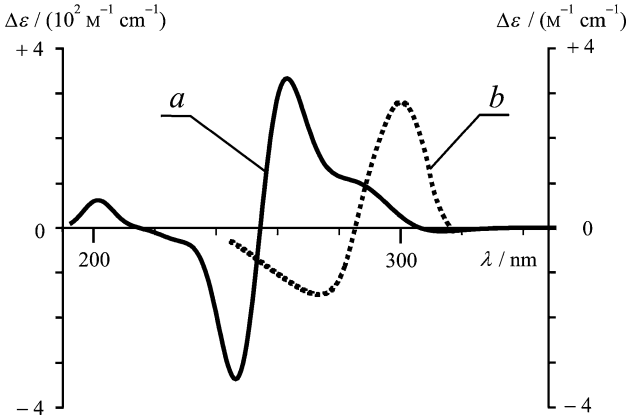

Fig. 3 CD of Λ-$[Si(acac)_3]^+$. *a*: calculated using B3LYP functional and 6-31G basis; *left scale*. *b*: experimental CD of Λ-$[Si(acac)_3]^+$ as the mirror image of that given in ref.4; *right scale*

Table 2 Λ-$[Si(acac)_3]^+$. A list over the lowest lying transitions with the computed energies, rotational strengths (The cgs unit for R is 10^{-40} Fr cm erg/G), and the dominating origins calculated with B3LYP/(6–31g)

State	Symmetry	E/eV	$E/\mu m^{-1}$	λmax/nm	$R*10^{40}$ Fr cm erg G^{-1}	Origin
19, 20	E	6.0414	4.87	205.22	85	$L_\sigma(e) \rightarrow 4\pi(a_1)$
17, 18	E	5.5146	4.45	224.83	2	$L_\sigma(a_2) \rightarrow 4\pi(e)$
16	A_1	5.4338	4.38	228.17	0	L_σ (e) $\rightarrow 4\pi(e)$
15	A_2	5.4175	4.32	231.5	−44	$L_\sigma(a_2) \rightarrow 4\pi(a_1)$
13, 14	E	5.3147	4.26	245.8	2	$L_\sigma(e) \rightarrow 4\pi(a_1)$
12	**A_2**	**4.9531**	**3.91**	**255.8**	**−907**	**$3\pi(e) \rightarrow 4\pi(e)$**
10, 11	**E**	**4.7849**	**3.79**	**264.2**	**454**	**$3\pi(a_2) \rightarrow 4\pi(e)$**
9	A_2	4.7849	3.77	265.0	−8	$L_\sigma(a_2) \rightarrow 4\pi(a_1)$
7, 8	E	4.6946	3.75	266.7	12	$L_\sigma(e) \rightarrow 4\pi(a_1)$
6	A_1	4.4689	3.75	278.4	0	$3\pi(e) \rightarrow 4\pi(e)$
4, 5	E	4.4051	3.53	283.3	62	$3\pi(a_2) \rightarrow 4\pi(e)$
2, 3	E	4.225	3.36	297.2	73	$3\pi(e) \rightarrow 4\pi(a_1)$
1	A_2	4.1254	3.27	305.5	−90	$3\pi(a_2) \rightarrow 4\pi(a_1)$
0	A_1	Ground state				

The three main components of the exciton transitions are pointed out with bold

nine substates written in a simplified notation are excited, non-diagonalized states with symmetries derived from Table 3 using the functions from the barred coordinate system.

$$
\begin{array}{ll}
|(3\pi e_x)^2(3\pi e_y)^2(3\pi a_2)(4\pi a_1)| & A_2 \\
|(3\pi e_x)^2(3\pi e_y)\,(4\pi a_1)\,(3\pi a_2)^2| & E_y \\
|(3\pi e_x)(4\pi a_1)\,(3\pi e_y)^2(3\pi a_2)^2| & E_x \\
|(3\pi e_x)^2(3\pi e_y)^2(3\pi a_2)(4\pi e_y)| & E_x \\
|(3\pi e_x)^2(3\pi e_y)(4\pi e_y)\,(3\pi a_2)^2| & A_1 \otimes E_x \\
|(3\pi e_x)(4\pi e_y)\,(3\pi e_y)^2(3\pi a_2)^2| & A_2 \otimes E_y \\
|(3\pi e_x)^2(3\pi e_y)^2(3\pi a_2)(4\pi e_x)| & E_y \\
|(3\pi e_x)^2(3\pi e_y)(4\pi e_x)\,(3\pi a_2)^2| & A_2 \otimes E_y \\
|(3\pi e_x)(4\pi e_x)(3\pi e_y)^2(3\pi a_2)^2| & A_1 \otimes E_x
\end{array}
$$

The $3\pi \rightarrow 4\pi$ transitions in three ligands around silicon(IV) in $[Si(acac)_3]^+$ must result in three transitions and not nine. The nine subfunctions should couple to the following three where the barred coordinate system is implicit:

$$
\begin{aligned}
\Psi(A_2) = \frac{1}{\sqrt{6}}[\,&|(3\pi e_x)^2(3\pi e_y)^2(3\overset{+}{\pi} a_2)(4\overline{\pi} a_1)| \\
&-|(3\pi e_x)^2(3\pi e_y)^2(3\overline{\pi} a_2)(4\overset{+}{\pi} a_1)| \\
&+|(3\overset{+}{\pi} e_x)(4\overline{\pi} e_y)\,(3\pi e_y)^2(3\pi a_2)^2| \\
&-|(3\overline{\pi} e_x)(4\overset{+}{\pi} e_y)\,(3\pi e_y)^2(3\pi a_2)^2| \\
&-|(3\pi e_x)^2(3\overset{+}{\pi} e_y)(4\overline{\pi} e_x)\,(3\pi a_2)^2| \\
&+|(3\pi e_x)^2(3\overline{\pi} e_y)(4\overset{+}{\pi} e_x)(3\pi a_2)^2|]
\end{aligned}
$$

$$
\begin{aligned}
\Psi(E_x) = \frac{1}{\sqrt{6}}[&|(3\overset{+}{\pi} e_x)(4\overline{\pi} a_1)\,(3\pi e_y)^2(3\pi a_2)^2| \\
&-|(3\overline{\pi} e_x)(4\overset{+}{\pi} a_1)\,(3\pi e_y)^2(3\pi a_2)^2| - (3\pi e_x)^2(3\pi e_y)^2 \\
&(3\overset{+}{\pi} a_2)(4\overline{\pi} e_y)| + |(3\pi e_x)^2(3\pi e_y)^2(3\overline{\pi} a_2)(4\overset{+}{\pi} e_y)| \\
&+\frac{1}{\sqrt{2}}(|(3\pi e_x)^2(3\overset{+}{\pi} e_y)(4\overline{\pi} e_y)\,(3\pi a_2)^2|-|(3\pi e_x)^2 \\
&(3\overline{\pi} e_y)(4\overset{+}{\pi} e_y)(3\pi a_2)^2|) - \frac{1}{\sqrt{2}}(|(3\overset{+}{\pi} e_x)(4\overline{\pi} e_x)\,(3\pi e_y)^2 \\
&(3\pi a_2)^2|-|(3\overline{\pi} e_x)(4\overset{+}{\pi} e_x)(3\pi e_y)^2(3\pi a_2)^2|)]
\end{aligned}
$$

$$
\begin{aligned}
\Psi(E_y) = \frac{1}{\sqrt{6}}[&|(3\pi e_x)^2(3\overset{+}{\pi} e_y)\,(4\overline{\pi} a_1)\,(3\pi a_2)^2|-|(3\pi e_x)^2 \\
&(3\overline{\pi} e_y)\,(4\overset{+}{\pi} a_1)\,(3\pi a_2)^2| + |(3\pi e_x)^2(3\pi e_y)^2 \\
&(3\overset{+}{\pi} a_2)(4\overline{\pi} e_x)|-|(3\pi e_x)^2(3\pi e_y)^2(3\overline{\pi} a_2)(4\overset{+}{\pi} e_x)| \\
&+\frac{1}{\sqrt{2}}(|(3\overset{+}{\pi} e_x)(4\overline{\pi} e_y)\,(3\pi e_y)^2(3\pi a_2)^2|-|(3\overline{\pi} e_x) \\
&(4\overset{+}{\pi} e_y)\,(3\pi e_y)^2(3\pi a_2)^2|) - \frac{1}{\sqrt{2}}(|(3\pi e_x)^2(3\overset{+}{\pi} e_y) \\
&(4\overline{\pi} e_x)(3\pi a_2)^2|-|(3\pi e_x)^2(3\overline{\pi} e_y)(4\overset{+}{\pi} e_x)(3\pi a_2)^2|)]
\end{aligned}
$$

A number of the commonly used functionals have been tested with these computations for correct symmetry adaption of π excited states. The results shown in Table 2 for TD DFT computations with the B3LYP are characteristic also for computations with XLYP, LSDA, B1B95LYP and TPPSh functional as illustrated in Fig. 4A. *Thus, these computations produce in principle wrong*

Table 3 Characterization of the TD-DFT computed $3\pi \rightarrow 4\pi$ transitions in $[Si(acac)_3]^+$ starting at low energy, transition 1, where Pop. refers to the population of various orbital transitions

Originating 3π orbital	Symmetry final 4π orbital	Symmetry	Pop.	Trans. no.	Final state
86	$A_2 \rightarrow 87$	A_1	0.66	1	$^1A_2$
85	$E\bar{y} \rightarrow 88$	$E\bar{x}$	−0.18	1	
84	$E\bar{x} \rightarrow 89$	$E\bar{y}$	−0.18	1	
85	$E\bar{y} \rightarrow 87$	A_1	0.63	3	$^1E\bar{x}$
84	$E\bar{x} \rightarrow 87$	A_1	0.63	2	$^1E\bar{x}$
86	$A_2 \rightarrow 89$	$E\bar{y}$	−0.27	2	
86	$A_2 \rightarrow 88$	$E\bar{x}$	0.52	4	$^1E\bar{y}$
85	$E\bar{y} \rightarrow 88$	$E\bar{x}$	−0.32	4	
84	$E\bar{x} \rightarrow 89$	$E\bar{y}$	0.32	4	
85	$E\bar{y} \rightarrow 87$	A_1	0.12	4	
86	$A_2 \rightarrow 89$	$E\bar{y}$	0.52	5	$^1E\bar{x}$
85	$E\bar{y} \rightarrow 89$	$E\bar{y}$	0.32	5	
84	$E\bar{x} \rightarrow 88$	$E\bar{x}$	0.32	5	
84	$E\bar{x} \rightarrow 87$	A_1	0.12	5	
84	$E\bar{x} \rightarrow 88$	$E\bar{x}$	−0.5	6	$^1A_1$
85	$E\bar{y} \rightarrow 89$	$E\bar{y}$	0.5	6	
84	$E\bar{x} \rightarrow 89$	$E\bar{y}$	−0.33	11	$^1E\bar{y}$
85	$E\bar{y} \rightarrow 87$	A_1	0.20	11	
85	$E\bar{y} \rightarrow 88$	$E\bar{x}$	0.33	11	
86	$A_2 \rightarrow 88$	$E\bar{x}$	0.33	11	
84	$E\bar{x} \rightarrow 87$	A_1	0.20	10	$^1E\bar{x}$
84	$E\bar{x} \rightarrow 88$	$E\bar{x}$	−0.33	10	
85	$E\bar{y} \rightarrow 89$	$E\bar{y}$	−0.33	10	
86	$A_2 \rightarrow 89$	$E\bar{y}$	0.34	10	
84	$E\bar{x} \rightarrow 89$	$E\bar{y}$	0.41	12	$^1A_2$
85	$E\bar{y} \rightarrow 88$	$E\bar{x}$	0.41	12	
86	$A_2 \rightarrow 87$	A_1	0.17	12	

results. The basis sets are in this respect of less significance. Figure 4B demonstrates that five long range functional all produce a correct coupling giving two components (E and A_2 transitions) under the $3\pi \rightarrow 4\pi$ ligand transitions. It may be worthwhile to mention that the distance from a middle carbon atom in one ligand is approximately 5.5 Å to the corresponding atom in another ligand.

With the appearance of Gaussian 09 long range functionals such as CAM-B3LYP and LC-wPBE have been introduced and these functionals have been found to work well for exciton coupled transitions as seen from Fig. 4 and Fig. 5 for calculated CD for Λ-$[Si(acac)_3]^+$ with LC-wPBE/cc-pVDZ. The long range functionals eliminate the incompletely coupled $3\pi \rightarrow 4\pi$ from the calculated states. We presume that only the long-range functionals allow the correct symmetrization of ligand orbitals and therefore also only they allow for a correct calculation of the electric and magnetic transition dipole moments.

We find that the use of a long range functional is important for standard DFT computations and that Gaussian 09 has filled an important gap for coordination compounds and hopefully for other extended systems as well. Thus, the similarity between the computed and the experimental CD reported in Fig. 5 is considered good. The energy offset of ca. 0.5 μm^{-1} is usual for TD-DFT results and the relative size of the two bands of the Cotton effect seems reasonable. However, the intensity of the CD seems to be overestimated by the computation. Even when one considers the optical resolution of $[Si(acac)_3]^+$ for incomplete it is difficult to believe that it could be so incomplete. Similar discrepancies are observed by other authors [16, 17]. Part of an explanation could be that the intensity is critically dependent of the splitting between the E and A_2 CD components due to mutual cancellation of the two gaussians. Actually, a small error in the calculation overestimating this energy difference will produce a very large intensity error.

The above reported calculation all refer to a gaseous state and as the CD was measured in aqueous solution one may expect an error that can be accounted for by using a solvation model. In Fig. 5 is shown the result of using the polarizable dielectric solvation model CPCM (also known

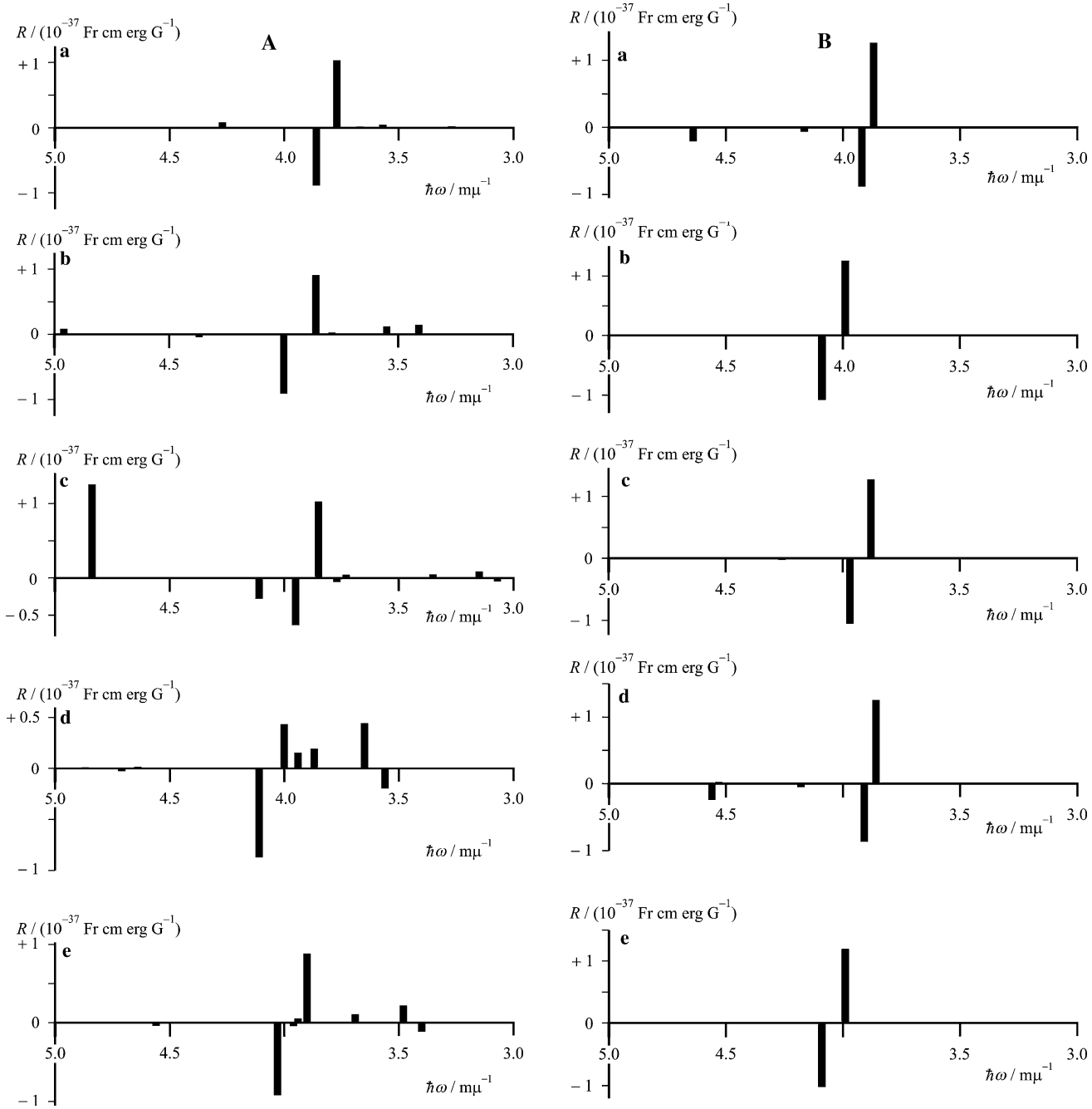

Fig. 4 **A** Computed rotatory strengths for Λ-$[Si(acac)_3]^+$ obtained with the basis 6-31G and the Gaussian functionals *a*: LSDA, *b*: B3LYP, *c*: TPSSh, *d*: B1B9LYP, and *e*: XB3LYP all showing a distribution of resulting transition states for the three HOMO to LUMO transitions in the ligands. **B** Computed rotatory strengths for Λ-$[Si(acac)_3]^+$ obtained with the basis cc-pVDZ and the Gaussian functionals *a*: wB97XD, *b*: LC-LSDA, *c*: LC-wPBE, *d*: CAM-B3LYP, and *e*: LC-BLYP all showing a correct distribution of results for the three HOMO to LUMO transitions in the ligands

as Cosmo). The change is relatively small but it does decrease the difference between the computed and the observed transition energies.

We can see that the TD DFT computation of CD for Λ-$[Si(acac)_3]^+$ is fundamentally better with a long range functional than with the conventional B3LYP, and it is only natural to see if other coordination ions of silicium(IV) could provide similar experience.

Tris(tropolonato)silicium(IV) ion, $[Si(trop)_3]^+$, tris(bipyridine) silicon(IV) ion, $[Si(bipy)_3]^{4+}$ and {2,2′,2″-[ethane-1,1,1-triyltris(methylenenitrilo-*N*-methanylylidene)]-triphenolato- *O*} silicon(IV) ion, $[Si(L)]^+$, are all dominated by internal ligand

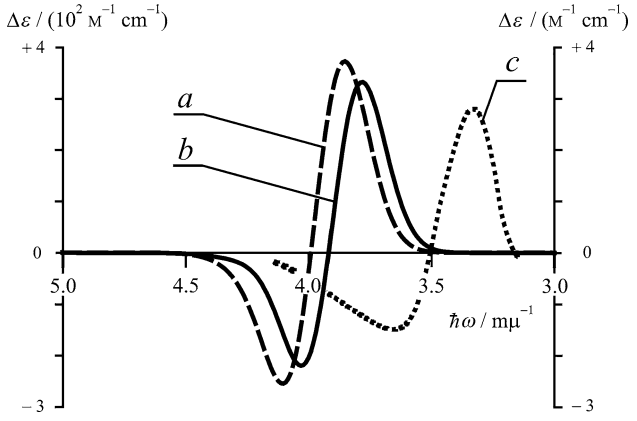

Fig. 5 CD of Λ-$[Si(acac)_3]^+$. *a*: Calculated using LC-wPBE/cc-pVDZ and gas condition; *left scale*. *b*: Calculated CD using LC-wPBE/cc-pVDZ and the solvation model CPCM (aqueous condition); *left scale c*: Experimental CD of Λ-$[Si(acac)_3]^+$; *right scale*

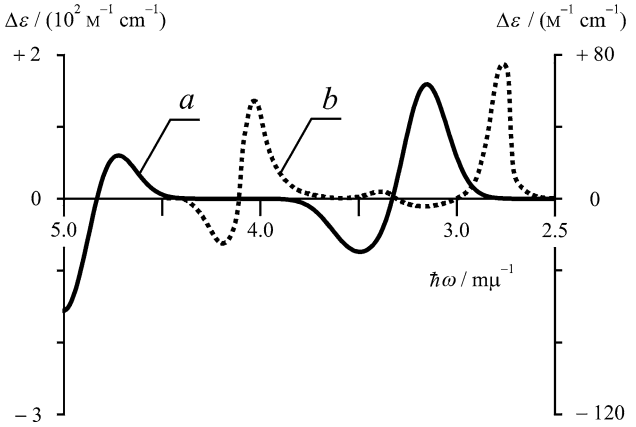

Fig. 6 CD for Λ-$[Si(trop)_3]^+$. *a*: calculated using LC-wPBE/cc-pVDZ (gas phase); *left scale*. *b*: experimental CD obtained from ref [3].; *right scale*

transitions with negligible charge transfer transitions and they have therefore also been selected for computations.

CD of (+)-$[Si(trop)_3]^+$ in ethanol was measured by Ito et al. [3]. Their assignment of the absolute configuration is confirmed by the TD-DFT computation and with the chosen functional, LC-wPBE, the correct coupling of the exciton transitions is achieved. The functional B3LYP introduces erroneously extra transitions in the long wavelength region as was seen for Λ-$[Si(acac)_3]^+$. The inclusion of the solvent model CPCM (ethanol) in this case causes an insignificant change. The overall similarity between the computed and the experimental CD spectra shown in Fig. 6 seems less satisfactory in this case but the energy offset is close to 0.5 μm^{-1} at low energies and only slightly higher at high energies.

The experimental CD spectrum for $[Si(bipy)_3]^{4+}$ has been measured by Yoshigawa's group at Okayama University [18]. It became interesting to study this silicon coordination compound because it is analogous to those transition metal ion complexes studied by Fan et al. [16, 19, 20]. The functional LC-wPBE gives a computed CD curve with the correct symmetry adaption of the $\pi \rightarrow \pi^*$ transitions. Figure 7 shows the experimental CD curve for $[Si(bipy)_3]^{4+}$ together with the computed CD for the functional LC-wPBE/ccPVDZ and using B3LYP/6-31G. In Table 4 is shown the long wavelength transitions computed with the functional B3LYP demonstrating the incorrect coupling with low energy components. These are not present in the results from calculation using the functional LC-wPBE. Thanks to the fact that we depict calculated spectra with a certain width such fundamental failures can be hidden and thus remain undetected.

The erroneous coupling with B3LYP functional is evident from the Fig. 7 and Table 4. It is also demonstrated by Fig. 7 and Table 4 bottom that a long range functional

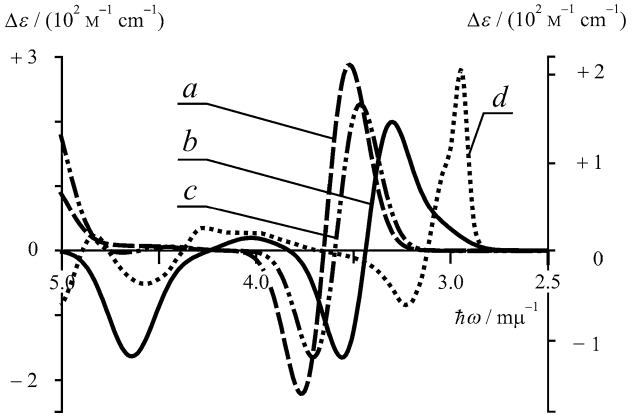

Fig. 7 CD for Λ-$[Si(bipy)_3]^{4+}$. *a*: computed with LC-wPBE/cc-pVDZ; *left scale*. *b*: computed with LC-wPBE/cc-pVDZ and the CPCM solvation model; *left scale*. *c:* computed using B3LYP/6-31G; left scale, and *d*: the experimental CD from ref [18].; *right scale*

gives a satisfactory calculation of the CD. The high charge for $[Si(bipy)_3]^{4+}$ suggests a larger difference between a gas phase computational results and results obtained with a solvation model. This is indeed seen using the CPCM model with water as solvent as shown in Fig. 7.

The cation of the complicated optically active Λ-{2,2′,2″-[ethane-1,1,1-triyltris(methylenenitrilo-*N*-methanylylidene)] triphenolato- *O*}silicon(IV) perchlorate, Λ-$[Si(L)]ClO_4$ has the structure shown in Fig. 8 [21]. The CD has been studied in Yoshikawa's group and the available CD is compared in Fig. 9 with CD computed from the functional LC-wPBE. Also for this coordination compound the B3LYP functional computes low energy rotatory strengths due to imperfect coupling.

Notice the important difference between the experimental CD and computed CD. There is a top at low energy in the experimental CD curve which cannot be accounted

Table 4 Top part shows results from a B3LYP CD calculation of $[Si(bipy)_3]^{4+}$ while the lower part shows results from a CD calculation with LC-wPBE

State	Excited state number	E/μm^{-1}	λ/nm	R/10^{40} Fr cm erg G^{-1}
				With B3LYP
A_1	16	4.1049	243.6	0
A_2	15	4.0332	247.9	0.00
E	13, 14	4.0332	247.9	0.04
A_2	12	4.0072	249.6	7.26
E	10, 11	3.9870	250.8	1.22
A_2	**9**	**3.4917**	**286.4**	**−567.75**
E	**7.8**	**3.3644**	**197.2**	**632.20**
E	5, 6	3.1755	314.9	304.18
A_2	4	3.1660	315.9	−338.91
E	2, 3	3.0873	323.9	127.50
A_1	1	3.0634	326.4	0
				With LC-wPBE
E	11,12	6.2775	199.6	10.23
A	10	5.0065	199.8	0.00
E	8,9	4.7213	211.8	4.48
A_2	7	4.7092	212.4	0.79
E	5, 6	4.4797	223.2	3.93
A_1	4	4.4394	225.3	0.00
A_2	**3**	**3.6738**	**272.2**	**−1139.66**
E	**1, 2**	**3.5915**	**278.5**	**636.91**

The exciton states are shown in bold

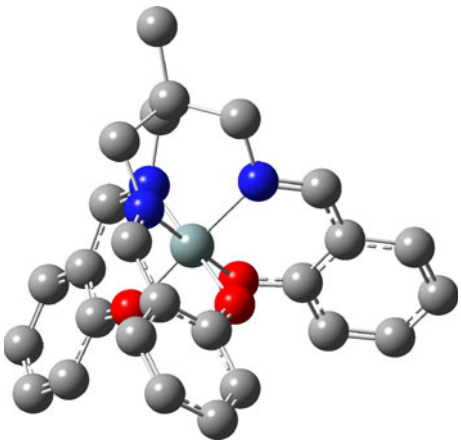

Fig. 8 {2,2′,2″-[ethane-1,1,1-triyltris(methylenenitrilo-*N*-methanylylidene)]-triphenolato-O}silicon(IV) cation (Si *green*, C *gray*, N *blue*, O *red*. H omitted for clarity)

for by the computations, since they inevitably suggest exciton split CD components from the HOMO → LUMO ligand transitions. However, if the computation overestimates the splitting between the E and A LUMO states one could to see if moving the CD belonging to A to the same energy as that of the E component. The mutual cancellation

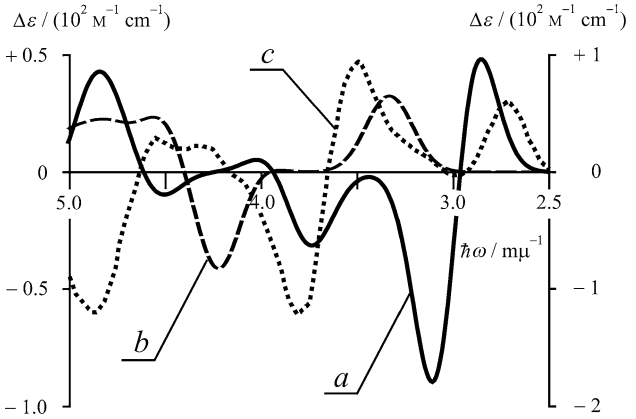

Fig. 9 CD for Λ-$[Si(L)]^+$. *a*: calculated CD using LC-wPBE/cc-PVDZ (gas phase); *left scale b*: CD calculated using LC-wPBE/cc-PVDZ (gas phase) and the artificial situation where the energy of the LUMO A_2 state is set equal to the energy of the LUMO E state; *left scale c*: the experimental curve from Ref. [21].; *right scale*

of the two CD components results in the CD shown in Fig. 9c and the low energy top now appears as a non-degenerate transition. The rest of the calculated CD curve has only little resemblance with the second and third components of the experimental CD and we find this example a puzzle.

Recently, TD DFT computations for $[Cr(acac)_3]$ and $[Fe(bipy)_3]^{2+}$ have appeared from Ziegler's group that has produced CD curves looking very similar to the experimental curves [16, 19]. In that work a local density approximation was used in combination with BP86 gradient corrections.

Acknowledgments We wish to thank University of Copenhagen for giving us working conditions for this project.

References

1. Larsen, E., Mason, S.F., Searle, G.H.: Absorption and circular dichroism spectra and absolute configuration of tris acetylacetonato silicon(IV) ion. Acta Chem. Scand. **20**, 191–196 (1966)
2. Dhar, S.K., Doron, V., Kirschner, S.: 6-Coordinate silicon(IV).2. The hydrolysis and racemization of the tris-(acetylacetonato)-silicon(IV) cation. J. Am. Chem. Soc. **81**, 6372–6375 (1959)
3. Ito, T., Tanaka, N., Hanazaki, I., Nagakura, S.: Absolute configuration and polarization of the ligand $\pi^* \leftarrow \pi$ transition of the tris(tropolonato)silicon(IV) ion. Inorg. Nucl. Chem. Lett. **5**, 781–782 (1969)
4. Adam, K.R., Atkinson, I.M., Lindoy, L.F.: Local density functional theory analysis of the structures and energies of the isomers of low-spin $[Ni(cyclam)]2^+$. Inorg. Chem. **36**, 480–481 (1997)
5. Hambley T, Lindoy, L.F., Reimers, J.R., Turner, P., Wei, G., Widmer-Cooper, A.N.: Macrocyclic ligand design. X-Ray, DFT and solution studies of the effect of *N*-methylation an *N*-benzylation of 1,4,10,13-tetraoxa-7,16-diazacyclooctadecane on its affinity ofor selected transition and post-transition metal ions. Dalton Trans., 614–620 (2001)

6. Heine, K.B., Clegg, J.K., Heine, A., Gloe, K., Henle, T., Bernhardt, G., Cai, Z.-L., Reimers, J.R., Lindoy, L.F., Lach, J., Kersting, B.: Complexation, computational, magnetic, and structural studies of the Maillard reaction product isomaltol including investigation of an uncommon πi interaction with copper(II). Inorg. Chem. **50**, 1498–1505 (2011)
7. Kapinos L.E., Operschall, B.P., Larsen, E., Sigel, H., Understanding the acid–base properties of adenosine. The intrinsic basicities of N1, N3, and N7. Eur. J. Chem. (2011). doi: 10.1002/chem.201003544
8. Thulstrup P.N., Broge L., Larsen E., Springborg J.: On the electronic structure and spectroscopic properties of a pseudo-tetrahedral cationic cobalt(II) tetraamine complex—([3(5)]adamanzane)cobalt(II). Dalton Trans., 3199–3204 (2003)
9. Thulstrup P.W., Larsen E.: The electronic structure and spectra of spin-triplet ground state bis(biuretato)cobalt(III) coordination compounds. Dalton Trans.,1784–1789 (2006)
10. Diedrich, C., Grimme, S.: Systematic investigation of modern quantum chemical methods to predict electronic circular dichroism spectra. J. Phys. Chem. A **107**, 2524 (2003)
11. Frisch, M.J., Trucks, G.W., Schlegel, H.B., Scuseria, G.E., Robb, M.A., Cheeseman, J.R., Scalmani, G., Barone, V., Mennucci, B., Petersson, G.A., Nakatsuji, H., Caricato, M., Li, X., Hratchian, H.P., Izmaylov, A.F., Bloino, J., Zheng, G., Sonnenberg, J.L., Hada, M., Ehara, M., Toyota, K., Fukuda, R., Hasegawa, J., Ishida, M., Nakajima, T., Honda, Y., Kitao, O., Nakai, H., Vreven, T., Montgomery Jr., J.A., Peralta, J.E., Ogliaro, F., Bearpark, M., Heyd, J.J., Brothers, E., Kudin, K.N., Staroverov, V.N., Kobayashi, R., Normand, J., Raghavachari, K., Rendell, A., Burant, J.C., Iyengar, S.S., Tomasi, J., Cossi, M., Rega, N., Millam, J.M., Klene, M., Knox, J.E., Cross, J.B., Bakken, V., Adamo, C., Jaramillo, J., Gomperts, R., Stratmann, R.E., Yazyev, O., Austin, A.J., Cammi, R., Pomelli, C., Ochterski, J.W., Martin, R.L., Morokuma, K., Zakrzewski, V.G., Voth, G.A., Salvador, P., Dannenberg, J.J., Dapprich, S., Daniels, A.D., Farkas, O., Foresman, J.B., Ortiz, J.V., Cioslowski, J., Fox, D.J.: Gaussian 09, Revision B.01. Gaussian, Inc., Wallingford, CT (2010)
12. Harnung, S.E., Ong, E.C., Weigang, O.E.: Low-resolution analysis of vibrational-electronic circular dichroism spectra. J. Chem. Phys. **55**, 5711–5724 (1971)
13. IUPAC: Nomenclature of Inorganic Chemistry. RCS Publishing Cambridge, Cambridge (2005)
14. Orgel, L.E.: Double bonding in chelated metal complexes. J. Chem. Soc., 3683–3686 (1961)
15. Dilthey, W.: Über Siliciumverbindungen. Berichte **36**, 923–930 (1903)
16. Fan, J., Seth, M., Autschbach, J., Ziegler, T.: Circular dichroism of trigonal dihedral chromium(III) complexes: a theoretical study based on open-shell time-dependent density functional theory. Inorg. Chem. **47**, 11656–11668 (2008)
17. Goerigk, L., Stefan, G.: Calculation of electronic CD spectra with time-dependent double-hybrid density functional theory. J. Phys. Chem. A **113**, 767–776 (2009)
18. Liu, H.L., Ohmori, Y., Kojima, M., Yoshikawa, Y.: Stereochemistry of six-coordinate octahedral silicon(IV) complexes containing 2,2′-bipyridine. J. Coord. Chem. **44**, 257–268 (1998)
19. Fan, J., Autschbach, J., Ziegler, T.: Electronic structure and circular dichroism of tris(bipyridyl) metal complexes within DFT. Inorg. Chem. **49**, 1355–1362 (2010)
20. Fan, J., Ziegler, T.: On the origin of circular dichroism in trigonal dihedral cobalt (III) complexes of unsaturated bidentate Ligands. Inorg. Chem. **47**, 4762–4773 (2008)
21. Kojima, M., Azuma, S., Hirotsu, M., Nakajima, K, Nanoyama, M., Yoshikawa, Y.: Optical Resolution of a six-coordinate silicon(IV) complex with a tripod hexadentate ligand. Chem. Lett. 482–483 (2000)